Journal of Medicinal Chemistry Article

J. Med. Chem. **2011,** *54,* 611–621 **611**
DOI: 10.1021/jm101394n

Synthesis, Physicochemical Characterization, and Biological Activities of New Carnosine Derivatives Stable in Human Serum As Potential Neuroprotective Agents

Massimo Bertinaria,[†] Barbara Rolando,[†] Marta Giorgis,[†] Gabriele Montanaro,[†] Stefano Guglielmo,[†] M. Federica Buonsanti,[†,∥] Valentina Carabelli,[‡] Daniela Gavello,[‡] Pier Giuseppe Daniele,[§] Roberta Fruttero,[†] and Alberto Gasco*[,†]

[†]*Dipartimento di Scienza e Tecnologia del Farmaco, Università degli Studi di Torino, Via Pietro Giuria 9, 10125 Torino, Italy,* [‡]*Dipartimento di Neuroscienze, Università degli Studi di Torino, Corso Raffaello 30, 10125 Torino, Italy, and* [§]*Dipartimento di Chimica Analitica, Università degli Studi di Torino, Via Pietro Giuria 5, 10125 Torino, Italy.* [∥] *Present address: CRB Bracco Imaging SpA, c/o Biondustry Park del Canavese, via Ribes 5, Colleretto Giacosa (TO) Italy.*

Received October 27, 2010

The synthesis and the physicochemical and biological characterization of a series of carnosine amides bearing on the amido group alkyl substituents endowed with different lipophilicity are described. All synthesized products display carnosine-like properties differentiating from the lead for their high serum stability. They are able to complex Cu^{2+} ions at physiological pH with the same stoichiometry as carnosine. The newly synthesized compounds display highly significant copper ion sequestering ability and are capable of protecting LDL from oxidation catalyzed by Cu^{2+} ions, the most active compounds being the most hydrophilic ones. All the synthesized amides show quite potent carnosine-like HNE quenching activity; in particular, **7d**, the member of the series selected for this kind of study, is able to cross the blood−brain barrier (BBB) and to protect primary mouse hippocampal neurons against HNE-induced death. These products can be considered metabolically stable analogues of carnosine and are worthy of additional investigation as potential neuroprotective agents.

Introduction

Carnosine, β-alanyl-L-histidine (**1**) (Chart 1), is a naturally occurring dipeptide that in humans is preferentially localized in skeletal muscles and brain.[1] Carnosine can display a variety of physiological roles, including that of a cytosolic buffering agent, that of a regulator of content of transition metal ions in biological fluids and tissues, owing to its ability to form complexes with these ions, and that of a regulator of macrophage function.[2−4] It is a potent scavenger of both reactive oxygen species (ROS[a]) and reactive nitrogen species (RNS), which induce peroxidation of unsaturated lipids present in membranes as well as of toxic reactive α,β-unsaturated aldehydes deriving from this oxidation.[1,5−8] Acrolein, 4-hydroxy-*trans*-2,3-nonenal (HNE), and malondialdehyde are examples of such products. They are potent bifunctional electrophiles able to bind nucleophilic centers present in both DNA and proteins. In addition, the second electrophilic center may undergo additional attack, affording protein−protein and DNA−protein cross-linking. The final result is an amplification of the cellular damage induced by oxidative attack on membranes. Another source of cellular damage is the glycation of proteins, namely the process whereby reducing sugars react with protein amino groups generating Schiff's bases. These latter products, in turn, can afford advanced glycation end products (AGEs) able to incorporate additional proteins through stable cross-links.[9] AGEs are toxic for those cells that are able to recognize them. Carnosine is capable of protecting proteins against glycation and of reacting with protein carbonyl groups to form carnosylated proteins.[10−12] Because ROS, RNS, lipidic oxidation, and glycation products may contribute to the development of many neurodegenerative and cardiovascular diseases, today there is a great interest in carnosine and related structures as potential therapeutic tools.

It is known that carnosine is rapidly cleaved to its constituents, histidine and β-alanine, by the carnosinases, which are a group of ubiquitous dipeptidases belonging to the family of metalloproteases. So far, two principal isoforms of carnosinase are known, one is a cytosolic form (EC 3.4.13.3) and the other (EC 3.4.13.20) is known as serum carnosinase because it is mostly present in the plasma and brain.[13,14] The facility of enzymatic hydrolysis of carnosine and of many related compounds limits their therapeutic potential. The nature of the metal ion in serum carnosinase is not known with precision, but it is likely that two Zn^{2+} ions are present in the catalytic site. A recent computational study shows that one of these two ions is important in recognizing the carboxylic group of carnosine.[15] If this interaction is lost, it is reasonable to think that the affinity for the enzyme is strongly reduced. By contrast, the carboxylic group of carnosine should be less involved in recognition of the binding site of hPepT1, which is

*To whom correspondence should be addressed. Phone: +39 011 6707670. Fax: +39 011 6707286. E-mail: alberto.gasco@unito.it.

[a] Abbreviations: AGEs, advanced glycation end products; HNE, 4-hydroxy-*trans*-2,3-nonenal; RCS, reactive carbonyl species; ROS, reactive oxygen species; RNS, reactive nitrogen species; LDL, low density lipoprotein; HBTU, *O*-Benzotriazol-1-yl-*N*,*N*,*N*′,*N*′-tetramethyluronium hexafluorophosphate; HOBt, 1-hydroxybenzotriazole; DIPEA, di-isopropylethylamine; DMF, dimethylformamide; DCC, dicyclohexylcarbodiimide; TBARS, thiobarbituric acid reactive substances; hPepT1, human PepT1 transporter.

Published on Web 12/23/2010

Chart 1. β-Alanyl-L-histidine (Carnosine)

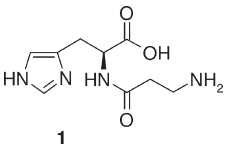

1

Scheme 1. Preparation of Carnosine Carbonamides **7a**−**n**[a]

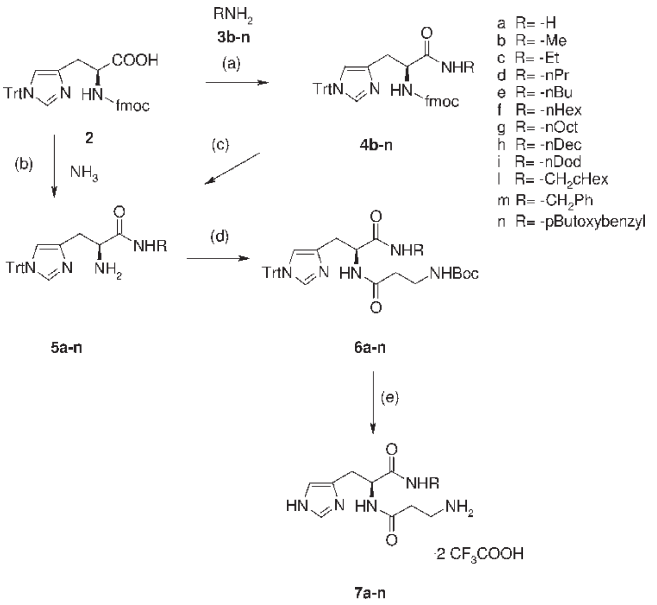

2 **4b-n** **5a-n** **6a-n** **7a-n**

[a] Reagents and conditions: (a) DIPEA, HBTU, $HOBt_{cat}$, 10 min rt, then **3b**−**n** 1−18 h, rt; (b) DIPEA, HBTU, $HOBt_{cat}$, 10 min rt then NH_3 1 h, rt; (c) piperidine, dry DMF, 1 h, rt; (d) Boc-β-Ala(OH), DCC, dry CH_2Cl_2, 0 °C to rt 2−18 h; (e) CF_3COOH 10% in CH_2Cl_2, 20 h, rt.

the main intestinal transporter involved in the absorption of both dietary peptides and peptidomimetics.[16]

On these bases, we designed a series of carnosine carbonamide derivatives bearing on the amide nitrogen alkyl or aryl groups characterized by different lipophilicity (compounds **7a**−**n**). This paper reports synthesis, dissociation constants and lipophilicity determination, the ability to complex Cu^{2+} ions, and the stability in human serum of these products. Their capacity to inhibit human LDL autoxidation induced by Cu^{2+} and to sequester HNE, chosen as a model of reactive carbonyl species (RCS), is also considered. Finally, the ability to cross the BBB in an in vivo rat model and the cytoprotective efficacy on primary mouse hippocampal neurons is shown in the case of **7d**, one of the most promising members of the series.

Results and Discussion

Chemistry. The synthetic pathway used to prepare compounds **7a**−**n** is reported in Scheme 1. The commercially available N^{α}-fluorenylmethoxycarbonyl-*N*-trityl-L-histidine (Fmoc-His(Trt)-OH) (**2**) was coupled with the appropriate amines **3b**−**n** using the *O*-benzotriazol-1-yl-*N*,*N*,*N*′,*N*′-tetramethyluronium hexafluorophosphate (HBTU)/1-hydroxybenzotriazole (HOBt)/di-isopropylethylamine (DIPEA) protocol to obtain the corresponding intermediate amides **4b**−**n**. Fmoc deprotection with piperidine in DMF was achieved at room temperature (rt) to afford the expected amines **5b**−**n**. The simple amido derivative **5a** was obtained directly by action of ammonia on **2**. Free amines so obtained were coupled with *tert*-butoxycarbonyl protected β-alanine (Boc-β-Ala(OH)) using dicyclohexylcarbodiimide (DCC) as the coupling agent and then deprotected using 10% (v/v) CF_3COOH in CH_2Cl_2 at rt to afford the expected ditrifluoroacetates **7a**−**n**. In Scheme 2, the synthetic pathway followed for the preparation of the ether **12** that was used for a comparison in the Cu^{2+} complexing studies is reported. Dityrityl protected alcohol **8**[17] underwent Williamson etherification with ethylbromide in the presence of an excess of NaH in dry DMF, giving intermediate **9**. Selective detritylation of this product carried out using 1% (v/v) CF_3COOH in CH_2Cl_2 at 0 °C afforded the expected free amine **10**. This intermediate was coupled with Boc-β-Ala(OH), by the usual DDC-mediated procedure, obtaining **11**. Removal of the protecting groups was achieved with 10% (v/v) CF_3COOH in CH_2Cl_2 to afford the target compound **12**.

Scheme 2. Preparation of Carnosine Ethylether **12**[a]

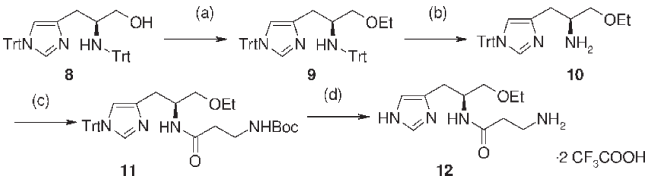

8 **9** **10** **11** **12**

[a] Reagents and conditions: (a) NaH, dry DMF, 1 h, rt, then EtBr 18 h, rt; (b) CF_3COOH 1% in CH_2Cl_2, 0 °C, 2 min; (c) Boc-β-Ala(OH), DCC, dry CH_2Cl_2, 0 °C to rt, 18 h; (d) CF_3COOH 10% in CH_2Cl_2, 20 h, rt.

Table 1. Dissociation Constants and Lipophilicity Parameters for Carnosine, **7a**−**n**, and **12**

compd	pK_{a1}[a]	pK_{a2}[a]	pK_{a3}[a]	Clog $D^{7.4}$[b]	Log $D^{7.4}$[c]
carnosine[d]	2.60	6.79	9.42	ND	ND
7a		6.17	9.16	−4.68	ND
7b		6.18	9.19	−4.35	ND
7c		6.17	9.16	−3.81	ND
7d		6.18	9.19	−3.30	−2.72
7e		6.18	9.19	−2.78	−2.01
7f		6.21	9.18	−1.72	−0.88
7g		6.21	9.18	−0.66	−0.23
7h		6.17[e]	9.21[e]	0.39	0.85
7i		6.16[e]	9.20[e]	1.46	0.93
7l		6.19	9.20	−1.73	−0.94
7m		6.22	9.19	−2.49	−1.76
7n		6.19	9.20	−0.99	−0.13
12		6.60	9.18	−2.88	−2.17

[a] Determined by potentiometric titration with GLpKa apparatus; $n \geq 4$, SD < 0.03. [b] Calculated according to the equation Clog $D^{7.4}$ = CLOGP − log [1 + $10^{(pKa_3-pH)}$ + $10^{(pKa_3-pKa_2-2pH)}$]; CLOGP for windows, v.1.0 Biobyte Corp., Claremont, CA, USA. [c] Determined by shake-flask technique; $n \geq 6$, SD < 0.2. [d] Reported values are in agreement with those reported in literature[28] (pK_{a1} = 2.59, pK_{a2} = 6.77, pK_{a3} = 9.37). [e] Data obtained with 20−34% methanol as cosolvent; aqueous pK_a values were obtained by extrapolation at 0% methanol using the Yasuda−Shedlovsky procedure.[51] ND = not determined.

Dissociation Constants (pK_as) and Lipophilicity. Dissociation constants (pK_as) of the new carnosine carbonamides and of ether derivative **12** were determined by potentiometric titration in aqueous solution using a GLpKa apparatus. Their values are collected in Table 1, with those of carnosine measured in the same conditions. For solubility reasons, in the case of compounds **7h** and **7i**, the measurements were carried out using methanol as a cosolvent and the results were extrapolated to zero cosolvent. As expected, pK_a values of imidazole rings lie in a very narrow range, just a little lower than the value of the carnosine imidazole ring. The values of the dissociation constants of the basic center in the lateral

chain are the same, within the experimental errors. At physiological pH (7.4), all the products exist prevalently as a mixture of monocharged and dicharged cations, unlike carnosine, which is a mixture of a zwitterion and a tricharged ion (++−).

The lipophilicity studies were carried out by shake-flask technique using as partition pair buffered water (pH 7.4)/*n*-octanol. The obtained distribution coefficients (log $D^{7.4}$) are reported in Table 1. The very high hydrophilicity of the compounds **7a**−**c** prevented the direct measurement of their log $D^{7.4}$. Consequently, these molecular descriptors were calculated from the related pK_a and CLOGP values (CLOGP for windows, v.1.0 Biobyte Corp., Claremont, CA, USA). As shown in Table 1, the lipophilicity of the series is modulated over a very large range (about 5.5 log units). As expected, it increases in the aliphatic series with the length of the chain: the simple amide **7a** is the most hydrophilic member and its dodecyl derivative **7i** the most lipophilic.

Stability in Human Serum. As aforementioned, carnosine is rapidly hydrolyzed by carnosinases. Therefore, one of the aspects that must be addressed when working with potential drugs structurally related to carnosine is their metabolic stability. A number of structural modifications of carnosine were carried out in order to obtain products with higher stability in biological media. The most common approach to obtain carnosinase-stable derivatives consisted in the removal of the carboxylic group from carnosine structure, thus obtaining β-alanylhistamine (carcinine). Carcinine and some of its N-substituted derivatives proved stable to enzymatic hydrolysis and were endowed with free radical scavenging ability.[18,19] Other modifications have regarded the peptide bond present in the parent molecule which was transformed into a sulfonamide, affording derivatives stable to carnosinase activity.[20] Acetylation on primary amine afforded the prodrug derivative *N*-acetylcarnosine, which proved more stable to carnosinase activity than parent L-carnosine,[13,19] moreover, substitution of the β-alanyl moiety with 2,3-diamino propionic acid, with different degrees of *N*-acetylation, afforded carnosinase stable compounds which were able to exert protective action against hydroxyl radical and peroxynitrite anion.[21] The inversion of configuration of the COOH group switching from L- to D-carnosine proved a successful approach. D-Carnosine and some synthesized derivatives were stable to hydrolysis in human serum and shared some common features with natural L-carnosine; in particular, D-carnosine was able to inhibit α-crystallin fibrillation and of disassembling α-crystallin amyloid fibrils.[22] Some D-carnosine analogues showed efficient sequestering of RCS.[23] Surprisingly enough, only a few approaches involving carnosine COOH group manipulation have been reported so far. In particular, amide formation with β-cyclodextrin affording carnosinase stable macromolecules endowed with antioxidant properties in different biological media was reported.[24,25] Other fluorinated amphiphilic alkylamides were synthesized and proposed as metal coordinating agents, however, their stability against carnosinase activity was not tested.[26] Carnosine and the carnosine amides **7a**−**n** were studied by RP-HPLC for their stability in human serum at 37 °C. Unlike the lead ($t_{1/2}$ = 5 min), all the products were completely stable over 3 h. This result is in keeping with the previously mentioned hypothesis that the carnosine carboxylic group binds a Zn^{2+} ion present in the active cleft of the enzyme, so playing a paramount role in the hydrolysis of the substrate.

Copper Complexes. Carnosine is able to form complexes with a number of metals. This property has been widely studied, and the complexes with Cu^{2+} have received particular attention in view of their physiological roles.[27,28] At neutral pH values at 35 °C, when the molar concentrations of carnosine and Cu^{2+} are equal, the predominant complex is represented by the neutral dimeric species $[Cu_2L_2H_2]^0$. A structure in solution related to the structure found in the solid state has been proposed for this complex, namely two Cu^{2+} ions, each bound to an amino group, dissociated amido function, N^3 imidazole nitrogen, and carboxylate oxygen.[29] Compounds **7a**, **7d**, **7g**, **7l**, and **7m** were chosen as representative members of the structural variety of carnosine amides here described to investigate the capacity of complexing Cu^{2+} of the series. Compound **12** and carnosine were also studied for comparison. The complex formation between copper(II) and the different carnosine derivatives has been investigated by means of the classical pH-metric technique. The stability constants of complexes have been expressed by $\beta_{pqr} = [Cu_pL_qH_r]/[Cu]^p[L]^q[H]^r$ (for reaction $pCu + qL + rH = Cu_pL_qH_r$, where L is the carnosine derivative, p, q, and r are the stoichiometric coefficients and charges are omitted for sake of simplicity). It must be pointed out that for ligands here studied, the dissociation of both peptide and amide hydrogens takes place at pH values too high to allow a reliable evaluation of the relative pK_a in aqueous solution. As a consequence, the concentration [L] in the expression of β_{pqr} takes into account only the hydrogen ion dissociation from protonated imidazole and amino nitrogens. If the presence of a metal ion promotes further dissociation of hydrogen ion from peptide and amide group, in the above reaction, the species H^+ is subtracted and the index r becomes negative. Thus, for all the complexes for which dissociation takes place from peptides and/or amide groups, the r index is negative. The measurements were carried out at t = 25 °C and ionic strength I = 0.15 M. The elaboration of experimental pH-metric data, in order to calculate the values of formation constants, has been performed by BSTAC program.[30] The results are listed in Table 2. From an inspection of these data, it can be observed that for all derivatives in which the carboxylate group has been transformed into amido or an N-substituted amido group, the stoichiometry of complexes is the same as for carnosine, but the stability is always significantly lower. This indicates that the contribution of carboxylate to the formation of the different species is more relevant if compared to that of amido group; moreover, the different N-substituents on amido group does not affect to a great extent the stability of copper(II) complexes. The stability of 11−1 complex ($\log\beta_{11-1}$ = 0.16) for the ligand **12**, which does not contain an amido group, is further lowered with respect to all the other ligands studied and, in addition, **12** does not form dimeric species, suggesting a participation, however, less significant with respect to carboxylate, of an amido group in the complex formation for all the above ligands (a weak coordination by carbonyl in 22−2 species and a more significant coordination by deprotonated amido group in 22−3 or 22−4 species). It is very likely that the structures of 22−2, 22−3, and 22−4 are similar to that reported for carnosine.[28]

The stability constants of Table 2 allow us to calculate the species distribution for the different complexes and the ratio between the free and total copper(II) concentration. If assuming $[Cu]_{total} = 2.5 \times 10^{-6}$ M and $[carnosine]_{total} = 1 \times 10^{-4}$ M, the values of $\log([Cu]_{total}/[Cu]_{free})$ at pH 7.4,

Table 2. Formation Constants ($\log \beta_{pqr}$)[a] of Copper(II) Complexes for Carnosine and Derivatives **7a**, **7d**, **7g**, **7l**, **7m**, **12**, and Logarithm of the Ratio between $[Cu^{2+}]_{total}$ and $[Cu^{2+}]_{free}$

compd	$\log \beta_{111}$	$\log \beta_{110}$	$\log \beta_{11-1}$	$\log \beta_{22-2}$	$\log \beta_{22-3}$	$\log \beta_{22-4}$	$\log \beta_{120}$	$\log ([Cu^{2+}]_{tot}/[Cu^{2+}]_{free})$ [b]
7a	12.62(5)	6.82(3)	1.15(8)	5.09(3)	−2.82(4)	−12.23(5)	13.86(4)	2.89
7d	12.22(4)	6.72(2)	1.25(7)	5.40(2)	−3.09(5)	−12.67(6)	13.47(4)	2.93
7g	12.47(5)	6.59(3)	1.55(6)	5.52(2)	−2.46(4)	−11.68(5)	13.81(4)	3.19
7l	12.71(4)	7.05(3)	1.53(7)	6.35(2)	−2.41(4)	−12.32(5)	13.27(4)	3.00
7m	12.69(5)	7.01(3)	1.50(7)	6.20(2)	−2.84(4)	−12.74(6)	13.26(4)	3.09
12	13.58(4)	7.30(2)	0.16(5)				13.30(4)	1.95
carnosine	13.30[c]	8.47[c]	2.44[c]	8.35[c]			14.05[d]	3.80

[a] In parentheses errors ($\pm 3\sigma$) in the last significant figures. [b] Calculated for $[Cu^{2+}]_{total} = 2.5 \times 10^{-6}$ M and $[ligand]_{total} = 1 \times 10^{-4}$ M at pH 7.4. [c] According to lit.[28] [d] According to lit.[53]

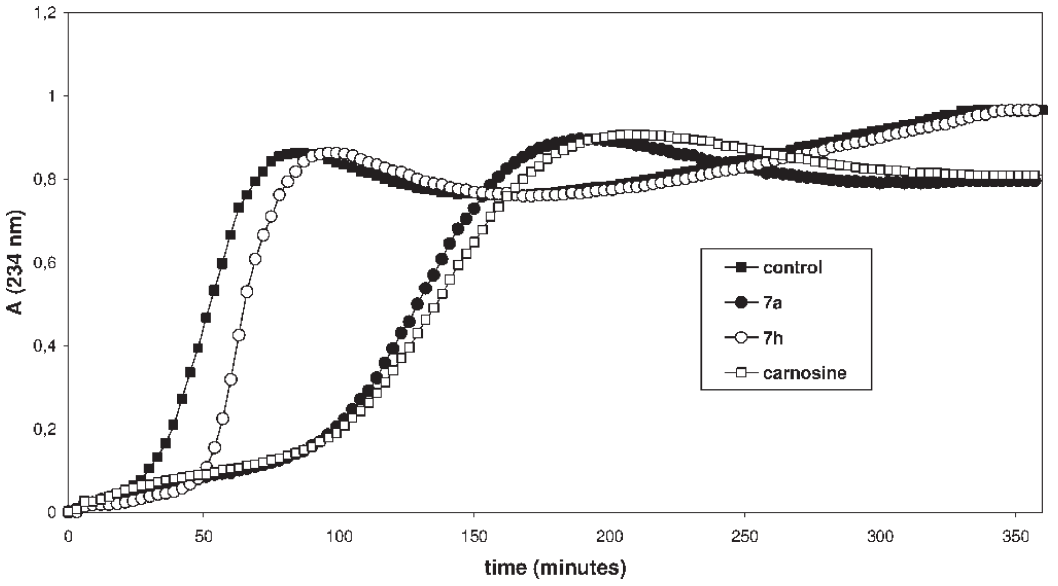

Figure 1. Effect of carnosine and compounds **7a** and **7h** on kinetics of conjugated diens formation during copper-induced LDL oxidation. The figure shows typical experimental kinetic profiles obtained by incubating the compounds (100 μM) at 37 °C with 50 μg mL^{-1} of LDL in PBS in the presence of 2.5 μM $CuSO_4$. Conjugated diene formation was assessed monitoring over 6 h the changes in absorbance at 234 nm.

range from 2.89 to 3.19 for all carnosine derivatives (Table 2). These values, if compared with the value calculated for carnosine (3.80), clearly indicate that, although it is weaker than that in lead, the sequestering ability of all the above ligands is highly significant. The value of $\log([Cu]_{total}/[Cu]_{free})$ is significantly lower for **12** (1.95) in which a N-substituted amido group is not present.

Antioxidant Activity. Oxidative stress occurs in cells, tissues, and organs when the balance between the concentration of the prooxidant reactive species and the antioxidant capacity is broken in favor of the prooxidant forces. Oxidative stress is involved in many pathological processes including aging, cancer, chronic inflammation, diabetic complications, cardiovascular diseases, including atherosclerosis and stroke, as well as a number of neurodegenerative disorders.[31,32] In particular, there is strong evidence that LDL-oxidation is increased in neurodegenerative and cognitive impairing diseases such Alzheimer's disease (AD) and vascular dementia.[33−36] As aforementioned, carnosine displays antioxidant properties; in particular, it is reported that carnosine was able to increase lag time for TBARS appearance and reduce the maximal rate of LDL oxidation catalyzed by Cu^{2+}. In the same work, conflicting results were obtained when hydroperoxides formation was monitored.[37] In our work, we tested carnosine and all the newly synthesized amides **7a**−**n** (100 μM) for their ability to suppress conjugated dienes formation during copper-mediated LDL (50 μg protein mL^{-1}) oxidation. The time course of autoxidation, initiated by the addition of 2.5 μM $CuSO_4$, was followed spectrophotometrically by detecting the formation of conjugated dienes at 234 nm. Typical examples of such experiments are reported in Figure 1 for carnosine, the simple amide derivative **7a**, and its *n*-decyl analogue **7h**. According to literature,[38] three parameters were used to characterize the kinetics of LDL oxidation: the maximal accumulation of oxidation products (OD_{max}), the Δlag time (Δt_{lag}), i.e. the duration of the period prior to onset of rapid lipidic peroxidation (propagation phase) compared to the control, and the propagation rate of the oxidation (R). OD_{max} of all the amides was the same as the control. R and Δt_{lag} derived for each compound from the corresponding curves are collected in Table 3, together with those measured for carnosine and the control. Analysis of the data indicates that the more hydrophilic products **7a**−**f**, **l**−**n**, bearing shorter alkyl substituent groups or the cyclohexylmethyl and benzyl substituents, are able to reduce R with respect to the control in a manner similar to carnosine. By contrast, all the remaining more lipophilic members of the series behave similarly to the control, with the only partial exception of **7h**, which induced a slight increase of the propagation rate of the oxidation. Analysis of Δt_{lag} values again indicates an influence of lipophilicity. Hydrophilic compounds are the most active members of the series, showing a Δt_{lag} near that of carnosine, while the less hydrophilic ones display lower activity. When Δt_{lag} is plotted against $\log D^{7.4}$, the diagram of Figure 2 is obtained. It shows that the ability of

Table 3. Antioxidant Activity and HNE Scavenging Ability of Derivatives **7a**−**n**, **12**, and Carnosine

	antioxidant activity		HNE scavenging ability		
compd	Δt_{lag} (min) ± SEM [a]	R (nmol min^{-1} mg^{-1} LDL prot) ± SEM [a]	HNE scavenged (%) ± SEM [b] 1 h	HNE scavenged (%) ± SEM [b] 6 h	HNE scavenged (%) ± SEM [b] 24 h
carnosine	67 ± 2	5.8 ± 0.3	20.4 ± 1.7	59.6 ± 1.6	88.8 ± 1.6
7a	64 ± 3	7.7 ± 0.4	10.2 ± 1.7	31.6 ± 1.4	77.7 ± 1.7
7b	75 ± 2	6.8 ± 0.6	8.0 ± 1.6	35.2 ± 0.8	75.4 ± 2.4
7c	68 ± 3	7.0 ± 0.3	8.4 ± 1.0	32.9 ± 1.1	70.9 ± 2.2
7d	68 ± 2	7.7 ± 0.3	12.5 ± 1.9	42.7 ± 2.0	81.0 ± 1.6
7e	82 ± 6	5.7 ± 0.3	12.5 ± 1.7	36.2 ± 1.2	75.2 ± 1.3
7f	79 ± 3	6.7 ± 0.4	12.0 ± 1.0	35.4 ± 1.9	75.9 ± 2.3
7g	43 ± 2	11.8 ± 0.4	12.8 ± 2.3	49.7 ± 1.9	86.7 ± 1.8
7h	9 ± 5	21.0 ± 1.0	ND	ND	ND
7i	−3 ± 3	14.5 ± 0.2	ND	ND	ND
7l	85 ± 5	5.6 ± 0.1	12.8 ± 3.2	28.2 ± 2.8	62.5 ± 2.1
7m	85 ± 4	5.2 ± 0.2	7.2 ± 1.4	29.3 ± 1.6	72.8 ± 0.6
7n	49 ± 5	10.0 ± 0.3	8.8 ± 1.6	32.6 ± 1.6	80.7 ± 0.8
12	−4 ± 1	12.2 ± 0.4	17.9 ± 1.6	60.7 ± 1.2	86.2 ± 0.3

[a] Obtained by $CuSO_4$-induced human LDL oxidation assay in the presence of compounds at 100 μM. R values were calculated from ΔA_{234} as a function of time, using $\varepsilon_{234} = 29500\ M^{-1}\ cm^{-1}$ for conjugated lipid peroxides. For control LDL samples, $R = 12.1 \pm 0.5$ nmol min^{-1} mg^{-1} LDL prot. [b] Determined in phosphate buffer (pH 7.4, 1 mM) at 37 °C; HNE (50 μM), test compound (1 mM). Scavenging % was calculated according to the following formula: scavenging (%) = 100 − {[(amount of HNE left after t h in the presence of the scavenger)/(amount of HNE left after t h in the control)] × 100}. ND = not determined.

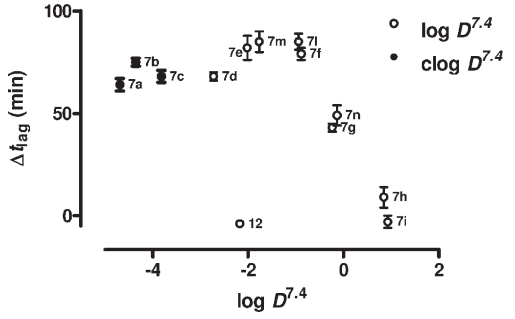

Figure 2. Relationship between antioxidant activity (expressed as Δt_{lag}) and log $D^{7.4}$ for carnosine amide derivatives **7a**−**n**; compound **12** is also showed for comparison.

carnosine amides to increase the lag time of the copper-catalyzed LDL peroxidation linearly increases with hydrophilicity and then reaches a plateau. It is known that Cu^{2+} ions can form LDL−copper complexes with binding sites of apolipoprotein, and the amount of copper bound to LDL increases with increasing concentrations of copper ions until the copper binding sites become saturated.[39] These complexes are able to produce free radicals at the LDL surface by interacting with preformed LDL-associated hydroperoxides (LOOH), thus inducing peroxidation.[40] As aforementioned, the ability of the amide analogues of carnosine to sequester Cu^{2+} ions at physiological pH is roughly similar. The lipophilicity of compounds, expressed by log $D^{7.4}$, should reasonably mimic their capacity of distribution between the LDL and the aqueous phase. Consequently, the linear tract of the plot in Figure 2 could be justified by the fact that, under the adopted experimental conditions, the higher the hydrophilicity is, the higher the amount of ligand in aqueous phase free to complex Cu^{2+} ions and thus able to decrease the onset of rapid lipidic peroxidation. Under the threshold log $D^{7.4}$ value of about −1.5, the amount of ligand sequestered by the LDL phase is so small that any further reduction of lipophilicity does not produce any appreciable variation in ligand aqueous concentrations and, consequently, in the amount of chelated Cu^{2+} ions; this could justify the presence of the plateau. The different ability to scavenge Cu^{2+} of the products as consequence of their different lipophilicity could also partly justify their different ability in influencing the propagation rate of the oxidation. Compound **12**, which does not contain amido group, was also tested for its ability to reduce LDL oxidation. It proved unable to modify the three parameters which characterize the kinetics of LDL oxidation. This result is in keeping with the very low Cu^{2+} sequestering ability shown by **12**.

HNE-Quenching Activity. The products formed by lipid peroxidation are degraded to reactive aldheydes such as HNE, malondialdehyde, and alkenals. HNE has been demonstrated to cause neuronal death.[41−44] Moreover HNE−protein adducts have been detected in the brain of patients with AD, therefore HNE is considered to play a crucial role in oxidative injury of biomolecules related to AD.[45−47] In the Introduction, we have already briefly discussed the biological role of carnosine as a quencher of α,β-unsaturated aldehydes. This reaction has been object of detailed studies.[6,7,48] Two adducts have been isolated as principal reaction products working in phosphate buffer, pH 7.4, using HNE as a model of reactive aldehyde. The former is an imidazole-based Michael adduct, stabilized as a five-membered cyclic hemiacetal and the latter a 13-membered ring Schiff base Michael adduct.[6,7,23,49] To evaluate whether carnosine amides display carnosine-like properties as quenchers of HNE, all the products were incubated in phosphate buffer, pH 7.4, with HNE at 37 °C. Samples relative to different incubation times were directly analyzed by RP-HPLC to measure HNE consumption. The % HNE quenched increased with the time and after 24 h reached a plateau. The results after 1, 6, and 24 h are summarized in Table 3. Carnosine, taken as reference, after 24 h was able to block about 89% of HNE. The most active product among the carnosine amides was the *n*-octyl substituted compound **7g**, which was as active as carnosine within the experimental error. For all the other compounds, the quenching effect on HNE fell in the range 62−81%. These results indicate that all

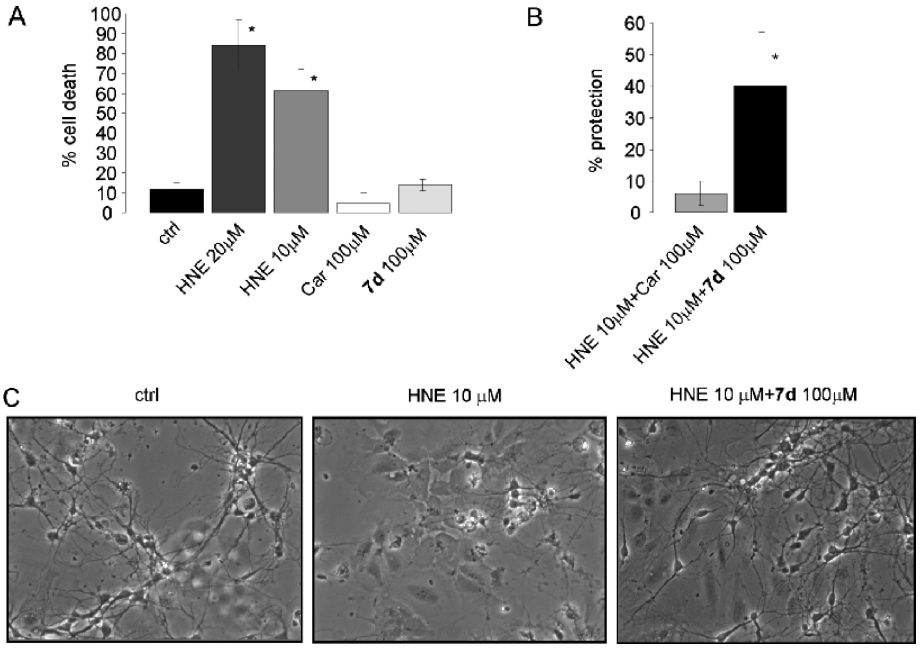

Figure 3. In vitro cytotoxicity on hippocampal neurons. (A) Percentage of cell death induced by different compounds on hippocampal neurons after 24 h exposure. (B) Percentage of cytoprotection after 24 h exposure of hippocampal cells to HNE (10 μM) and carnosine 100 μM (gray bar) or **7d** 100 μM (black bar). (C) Images at the optical microscope at 20× magnification. On the left, a group of control cells after 24 h. In the middle, a group of cell exposed for 24 h to HNE 10 μM. Cell death is evident. In the last panel, on the right, a group of cells after 24 h incubation with HNE 10 μM plus **7d** 100 μM. Reported results are given as mean ± SEM for n (n = 4−7) experiments. Statistical significance was calculated by using Student's paired t test. Values of $p < 0.05$ were considered significant.

the canosine amides here described display quite potent carnosine-like HNE quenching activity.

Protection from HNE-Induced Cell Death. On the bases of the results we obtained from the experiments of HNE-quenching activity, we decided to test the ability of compound **7d**, chosen as an example of this new series of carnosine derivatives, to protect primary mouse hippocampal neurons against HNE-induced death. Carnosine was taken as reference. At first, the adverse effects of **7d** (100 μM), HNE (10 and 20 μM), and carnosine (100 μM) on hippocampal neurons were evaluated (Figure 3A). Then, mouse hippocampal neurons were pretreated either with the selected compound or with carnosine and then exposed to HNE 10 μM concentration. After 24 h exposure, the percentage of cell death was evaluated (Figure 3B) by Trypan Blue exclusion in order to stain just dead cells due to loss of membrane integrity. Inspection of the Figure 3A indicates that, when compared to the control, HNE was able to kill 61−84% of treated cells in a concentration dependent manner while no adverse effect was seen either with carnosine or **7d**. Analysis of Figure 3B shows that carnosine has, if any, a very low cytoprotective efficacy (6 ± 4%), this is probably due to its instability to carnosinase, which is known to be present in mouse brain,[50] while **7d** triggers highly significant protective effect (40 ± 17%). Figure 3C shows the damage induced by HNE on the neural network (middle image) compared to the control (left image). The destruction is visible at the axonal level and also in the matrix surrounding the processes; moreover, there is a reduction in the total number of neurons and visible signs of necrosis. The presence of **7d** clearly reduces these effects (right image).

HPLC-Detection of 7d in Rat Serum and Brain. To further explore the neuroprotective potential of this class of compounds, we determined whether **7d** enters the brain by administering **7d** (20 mg/kg) intravenously to a group of rats. Blood and brain tissues samples were collected from rats assigned to 1.5 or 3 h post-treatment time points. Samples were analyzed by RP-HPLC (see Experimental Section), and concentration of **7d** was determined. At 3 h, the level of **7d** in brain was 1.1 ± 0.4 μg/g tissue, and at 1.5 h, the level of **7d** was about 0.6 μg/g tissue, approaching the detection limit of this technique. In blood, **7d** was only detectable at 1.5 h at a concentration of 0.26 μg/mL. The obtained data indicates how levels of **7d** in brain increased between 1.5 and 3 h of administration, whereas levels of **7d** in the serum decreased during this time interval.

Conclusion

This paper describes synthesis, physicochemical, and biological characterization of a series of carnosine amides bearing on the amido group alkyl substituents endowed with different lipophilicity. All the products were able to display carnosine-like properties, morover, they were stable over 3 h of incubation in human serum at 37 °C, unlike the lead that was rapidly cleaved into its constituents. All the synthesized compounds were capable of affording copper complexes at physiological pH with the same stoichiometry as carnosine and of displaying highly significant copper ion sequestering ability. The products were capable of protecting LDL from oxidation catalyzed by Cu^{2+} ions, the most active compounds being the most hydrophilic ones. All the amides triggered quite potent carnosine-like HNE quenching activity. **7d**, the compound chosen as the representative example of the series, was able to protect primary mouse hippocampal neurons against HNE-induced death. **7d** was also capable of penetrating rat brain after in vivo administration. These products can be considered metabolically stable analogues of carnosine, worthy of additional investigation as potential neuroprotective agents.

Experimental Section

Chemistry. Melting points were measured with a capillary apparatus (Büchi 540). Compounds **7a**−**h** and **12** were highly hygroscopic amorphous semisolids or foams. The determination of their melting point was affected by the complex thermal behavior of these compounds; consequently, the melting point was not reported. All the compounds were routinely checked by ^{1}H and ^{13}C NMR (Bruker Avance 300) at 300 and 75 MHz, respectively, and mass spectrometry (Finnigan-Mat TSQ-700). The following abbreviations are used to indicate the peak multiplicity: s = singlet, d = doublet, t = triplet, q = quartet, m = multiplet. Flash column chromatography was performed on silica gel (Merck Kieselgel 60, 230−400 mesh ASTM) using the reported eluents. Thin layer chromatography (TLC) was carried out on 5 cm×20 cm plates (Fluka) with a 0.2 mm layer thickness. Unless otherwise stated, anhydrous magnesium sulfate was used as the drying agent for the organic phases. Analysis (C, H, N) of the target compounds was performed by Service de Microanalyse, Université de Genève, Genève (CH), and REDOX (Monza), and the results were within ±0.4% of the theoretical. HNE (4-hydroxy-*trans*-2,3-nonenal) was prepared by acid treatment (1 mM HCl) of HNE-DMA (4-hydroxy-*trans*-2,3-nonenal-dimethylacetal; Sigma). Compound **8**[17] was synthesized according to the literature. Preparative HPLC was performed on a Lichrospher C_{18} column (250 mm×25 mm, 10 μm) (Merck Darmstadt, Germany) with a Varian ProStar mod-210 with Varian UV detector mod-325 with a flow rate of 39 mL/min; the detection was performed at 224 nm.

General Procedure for Preparation of 7a−n. To a stirred solution of Fmoc-His-(Trt)-OH (**2**) (2.5 g; 4 mmol) in dry DMF (40 mL), DIPEA (1.03 mL; 6 mmol), HBTU (2.29 g; 6 mmol), and HOBt (0.08 g; 0.6 mmol) were added. After 10 min, the appropriate amine **3a**−**n** (6 mmol) was added; the reaction mixture was allowed to stir at rt until TLC showed complete consumption of starting material (1−18 h). The solvent was removed under reduced pressure (oil pump) and the residue taken up with CH_2Cl_2 (40 mL) and washed with water (3×30 mL) and brine (30 mL), then dried and evaporated under reduced pressure. The residual oil was purified by flash chromatography eluting with CH_2Cl_2/MeOH 9.9/0.1 to 9.5/0.5 to afford the desired intermediate **4b**−**n** (56−100%). To a stirred solution of the obtained intermediate (2.59 mmol) in dry DMF (23 mL), piperidine (1.15 mL; 11.6 mmol) was added and the reaction mixture was stirred at rt for 1 h. The solvent was evaporated under reduced pressure, and the solid residue was taken up with CH_2Cl_2 (30 mL) and washed with water (3 × 30 mL) and brine (30 mL). The organic phase was dried (Na_2SO_4), and the crude product was purified by flash chromatography eluting with CH_2Cl_2/MeOH 9.8/0.2 to 8/2 to yield the desired intermediates **5b**−**n** (50−100%). When ammonia was used as the amine nucleophile in the coupling reaction with activated **2**, amidation and fmoc-deprotection were achieved in one step, leading to desired **5a**, which was isolated as a white solid after filtration from cold (0 °C) CH_2Cl_2 in 86% yield. To a stirred solution of the free amines **5a**−**n** (1.75 mmol) and Boc-β-Ala(OH) (0.35 g; 1.83 mmol) in dry CH_2Cl_2 (30 mL) kept at 0 °C, DCC (0.36 g; 1.75 mmol) was added, the ice bath was removed, and the reaction was stirred at rt for 2−18 h. The reaction mixture was cooled to 0 °C. The precipitate was filtered and washed with cold (0 °C) CH_2Cl_2. The liquid phase was washed with water (3 × 30 mL) and brine (30 mL) and then dried and evaporated under reduced pressure to leave a white solid. The crude material was purified by flash chromatography eluting with CH_2Cl_2/MeOH 9.8/0.2 to 9.5/0.5 to give the desired derivatives **6a**−**n** (41−98%) as white foams. The obtained products were dissolved in CH_2Cl_2 (21 mL), treated with CF_3COOH (2.1 mL), and stirred at rt for 20 h. The solvent was evaporated under reduced pressure, and the semisolid residue was treated with water (30 mL). The formed precipitate was filtered off through a sintered glass funnel, and the water phase was washed with CH_2Cl_2 (2 × 20 mL) and then with EtOAc (2 × 20 mL) and evaporated to afford the final product.

***β*-Alanyl-L-histidinamide Ditrifluoroacetate (7a).** The product was recrystallized from dry MeOH/Et_2O and freeze-dried to afford **7a** as an amorphous semisolid material; overall yield: 28%. ^{1}H NMR (DMSO): δ 8.81 (s, 1H, ImH_2), 8.46 (d, 1H, J = 8.4 Hz, N*H*CH), 7.86 (s, br, 3H, NH_3^+), 7.52 (s, br, 1H, CON*H*H), 7.28 (s, 1H, ImH_5), 7.26 (s, br, 1H, CONH*H*), 4.55−4.48 (m, 1H, C*H*), 3.17−2.85 (m, 4H, 2 CH_2), 2.61−2.43 (m, 2H, COCH_2). ^{13}C NMR (DMSO): δ 172.1, 169.7, 134, 130.3, 116.9, 51.8, 35.3, 32.2, 27.3.

***β*-Alanyl-*N*-methyl-L-histidinamide Ditrifluoroacetate (7b).** The product was recrystallized from dry MeOH/Et_2O and freeze-dried to afford **7b** as a white amorphous foam; overall yield 29%. ^{1}H NMR (DMSO): δ 8.89 (s, 1H, ImH_2), 8.52 (d, 1H, J = 8.1 Hz, N*H*CH), 8.03−8.01 (m, 1H, NHCH_3), 7.89 (s, br, 3H, NH_3^+), 7.30 (s, 1H, ImH_5), 4.56−4.49 (m, 1H, C*H*), 3.17−2.83 (m, 4H, 2 CH_2), 2.57 (d, 3H, J = 4.5 Hz, CH_3), 2.51−2.41 (m, 2H, COCH_2). ^{13}C NMR (DMSO): δ 170.1, 169.5, 134, 133.7, 116.6, 51.7, 35, 32, 27, 25.6.

***β*-Alanyl-*N*-ethyl-L-histidinamide Ditrifluoroacetate (7c).** The product was recrystallized from dry MeOH/Et_2O and freeze-dried to afford **7c** as a white amorphous foam; overall yield 78%. ^{1}H NMR (CD_3OD): δ 8.68 (s, 1H, ImH_2), 7.29 (s, 1H, ImH_5), 4.70−4.60 (m, 1H, C*H*), 3.21−3.04 (m, 6H, 3 CH_2), 2.66−2.64 (m, 2H, COCH_2), 1.10−1.06 (t, 3H, J=7.2 Hz, CH_3). ^{13}C NMR (CD_3OD): δ 172.3, 171.9, 135.1, 131.5, 118.3, 53.8, 36.8, 35.4, 32.7, 28.5, 14.7.

***β*-Alanyl-*N*-propyl-L-histidinamide Ditrifluoroacetate (7d).** The product was recrystallized from dry MeOH/Et_2O and freeze-dried to afford **7d** as a white amorphous foam; overall yield: 41%. ^{1}H NMR (DMSO): δ 8.84 (s, 1H, ImH_2), 8.50 (d, 1H, J = 8.4 Hz, N*H*CH), 8.06 (t, 1H, J = 10.8 Hz, CON*H*CH_2), 7.90 (s, br, 3H, NH_3^+), 7.28 (s, 1H, ImH_5), 4.57−4.50 (m, 1H, C*H*), 3.16−2.85 (m, 6H, 3 CH_2), 2.58−2.42 (m, 2H, COCH_2), 1.39 (q, 2H, J=7.2 Hz, CH_2CH$_3$), 0.91 (t, 3H, J=7.2 Hz, CH_3). ^{13}C NMR (DMSO): δ 170.5, 170.4, 134.6, 130.7, 117.6, 52.8, 41.3, 36, 32.9, 28.2, 23, 12.1.

***β*-Alanyl-*N*-butyl-L-histidinamide Ditrifluoroacetate (7e).** The product was recrystallized from dry MeOH/Et_2O and freeze-dried to afford **7e** as a white amorphous foam; overall yield 31%. ^{1}H NMR (CD_3OD): δ, 8.74 (d, 1H, J = 1.2 Hz, ImH_2), 7.30 (d, 1H, J = 1.2 Hz, ImH_5), 4.68−4.64 (m, 1H, C*H*), 3.30−3.02 (m, 6H, ImCH_2, NHCH_2, CH_2NH$_3^+$), 2.71−2.58 (m, 2H, COCH_2), 1.49−1.35 (m, 4H, CH_2CH_2), 0.93 (t, 3H, J=7.2 Hz, CH_3). ^{13}C NMR (CD_3OD): δ 172.3, 172, 135.1, 131.4, 118.4, 53.8, 40.3, 36.8, 32.7, 32.4, 28.41, 21, 14.1.

***β*-Alanyl-*N*-hexyl-L-histidinamide Ditrifluoroacetate (7f).** The product was purified by RP-HPLC eluting with MeOH/H_2O 60/40 + 0.1% TFA to give pure **7f** as a white amorphous foam; overall yield 49%. ^{1}H NMR (CD_3OD): δ 8.81 (s, 1H, ImH_2), 7.33 (s, 1H, ImH_5), 4.70−4.65 (m, 1H, C*H*), 3.31−3.03 (m, 6H, ImCH_2, NHCH_2, CH_2NH$_3^+$), 2.73−2.56 (m, 2H, COCH_2), 1.49−1.44 (m, 2H, NHCH$_2$CH_2), 1.33−1.28 (m, 6H, 3 CH_2), 0.90 (t, 3H, J = 6.9 Hz, CH_3). ^{13}C NMR (CD_3OD): δ 172.3, 171.9, 135, 131.1, 118.4, 53.7, 40.6, 36.8, 32.69, 32.66, 30.3, 28.3, 27.7, 23.6, 14.4.

***β*-Alanyl-*N*-octyl-L-histidinamide Ditrifluoroacetate (7g).** The product was recrystallized from dry MeOH/Et_2O and freeze-dried to afford **7g** as white amorphous foam; overall yield 41%. ^{1}H NMR (CD_3OD): δ 8.78 (s, 1H, ImH_2), 7.33 (s, 1H, ImH_5), 4.70−4.65 (m, 1H, C*H*), 3.30−3.08 (m, 6H, NHCH_2, ImCH_2, CH_2NH$_3^+$), 2.68−2.62 (m, 2H, COCH_2), 1.49−1.44 (m, 2H, NHCH$_2$CH_2), 1.30−1.28 (m, 10H, 5 CH_2), 0.90 (t, 3H, J=6.9 Hz, CH_3). ^{13}C NMR (CD_3OD): δ 172.3, 171.9, 135, 131.2, 118.4, 53.7, 40.7, 36.8, 33.0, 32.7, 30.42, 30.41, 30.36, 28.3, 28, 23.7, 14.5. ^{1}H NMR in agreement with those reported for the hydrochloride derivative.[26]

***β*-Alanyl-*N*-decyl-L-histidinamide Ditrifluoroacetate (7h).** The product was purified by RP-HPLC eluting with MeOH/H_2O 70/30 + 0.1% TFA to give **7h** as a white amorphous solid; overall

yield 29%. ^{1}H NMR (CD_3OD): δ 8.81 (s, 1H, ImH_2), 7.33 (s, 1H, ImH_5), 4.70−4.65 (m, 1H, CH), 3.34−3.03 (m, 6H, NHCH_2, ImCH_2, CH_2NH_3^+), 2.71−2.56 (m, 2H, COCH_2), 1.48−1.44 (m, 2H, NHCH$_2$CH_2), 1.31−1.29 (m, 14H, 7 CH_2), 0.90 (t, 3H, J = 6.9 Hz, CH_3). ^{13}C NMR (CD_3OD): δ 172.3, 171.9, 135, 131.2, 118.4, 53.7, 40.8, 36.8, 33.1, 32.7, 30.8, 30.7, 30.49, 30.46, 30.37, 28.3, 28, 23.8, 14.5. ^{1}H NMR in agreement with those reported for the hydrochloride derivative.[26]

β-Alanyl-*N*-dodecyl-L-histidinamide Ditrifluoroacetate (7i). The product was purified by RP-HPLC eluting with MeOH/H_2O 80/20 + 0.1% TFA to give the desired **7i** as a white amorphous solid; overall yield 14%; mp 72.2−80.7 °C. ^{1}H NMR (CD_3OD): δ 8.79 (s, 1H, ImH_2), 7.36 (s, 1H, ImH_5), 4.75−4.70 (m, 1H, CH), 3.26−3.02 (m, 6H, ImCH_2, NHCH_2, CH_2NH_3^+), 2.71−2.58 (m, 2H, COCH_2), 1.48−1.44 (m, 2H, NHCH$_2$CH_2), 1.30−1.29 (m, 18H, 9 CH_2), 0.90 (t, 3H, J = 6.9 Hz, CH_3). ^{13}C NMR (CD_3OD): δ 172.5, 172.1, 134.9, 131.1, 118.4, 53.9, 40.8, 36.8, 33.0, 32.7, 30.77, 30.75, 30.71, 30.6, 30.5, 30.4, 30.3, 28.7, 28, 23.7, 18.4.

β-Alanyl-*N*-cyclohexyl-L-histidinamide Ditrifluoroacetate (7l). The product was purified by RP-HPLC eluting with MeOH/H_2O 70/30 + 0.1% TFA and freeze-dried to give **7l** as a white amorphous solid; overall yield 37%; mp 74.5−84.2 °C. ^{1}H NMR (CD_3OD): δ 8.81 (s, 1H, ImH_2), 7.34 (s, 1H, ImH_5), 4.71−4.66 (m, 1H, CH), 3.30−2.94 (m, 6H, ImCH_2, NHCH_2cHex, CH_2-NH_3^+), 2.66−2.59 (m, 2H, COCH_2), 1.73−0.90 (m, 11H, cHex$H$). ^{13}C NMR (CD_3OD): δ 172.5, 172.2, 135.2, 131.3, 118.6, 54, 47.1, 39.3, 37.1, 32.9, 32.1, 28.5, 27.7, 27.2.

β-Alanyl-*N*-benzyl-L-histidinamide Ditrifluoroacetate (7m). The product was recrystallized from MeOH/Et_2O and freeze-dried to give **7m** as a white amorphous solid; overall yield 20%; mp 158.7−161.9 °C. ^{1}H NMR (CD_3OD): δ, 8.74 (s, 1H, ImH_2), 7.32−7.21 (m, 6H, ImH_5, 5 ArH), 4.76−4.71 (m, 1H, CH), 4.45−4.30 (m, 2H, NHCH_2), 3.20−2.95 (m, 4H, ImCH_2, CH_2NH_3^+), 2.76−2.58 (m, 2H, COCH_2). ^{13}C NMR (CD_3OD): δ 172.4, 172, 139.7, 134.9, 129.6, 128.6, 128.4, 118.42, 112.2, 53.8, 44.2, 36.8, 32.7, 28.1.

β-Alanyl-*N*-(4-butoxbenzyl)-L-histidinamide Ditrifluoroacetate (7n). The product was purified by preparative RP-HPLC eluting with MeOH/H_2O 60/40 + 0.1% TFA and freeze-dried to give the desired product as a white solid; overall yield 17%; mp 70.8−73.2 °C. ^{1}H NMR (CD_3OD): δ 8.73 (s, 1H, ImH_2), 7.23 (s, 1H, ImH_5), 7.10 (d, 2H, J = 8.7 Hz, Ar$H_{2',6'}$), 6.82−6.79 (d, 2H, J = 8.7 Hz, Ar$H_{3',5'}$), 4.67 (m, 1H, CH), 4.26−4.23 (m, 2H, NHCH_2), 3.91 (t, 2H, J = 6.3 Hz, OCH_2), 3.15−3.10 (m, 4H, ImCH_2, CH_2NH_3^+), 2.62−2.61 (m, 2H, COCH_2), 1.72−1.68 (m, 2H, CH$_2$CH_2CH$_2$CH$_3$), 1.47−1.45 (m, 2H, CH$_2$CH$_2$CH_2-CH$_3$), 0.94 (t, 3H, J = 7.2 Hz, CH_3). ^{13}C NMR (CD_3OD): δ 172.3, 171.8, 160, 134.9, 131.5, 131, 130, 118.4, 115.5, 68.7, 53.8, 43.7, 36.8, 32.7, 32.5, 28.2, 20.3, 14.2.

3-Amino-*N*-[(1*S*)-2-ethoxy-1-(1*H*-imidazol-4-ylmethyl)ethyl]-propanamide Ditrifluoroacetate (12). In a flame-dried flask equipped with a $CaCl_2$ guard tube, NaH 60% in mineral oil (0.83 g; 20.8 mmol) suspended in dry DMF (12.5 mL) was stirred for 1 h. A solution of **8** (2.50 g; 4.0 mmol) in dry DMF (15 mL) was added, and the reaction mixture was stirred at rt for 1 h, then bromoethane (1.09 g; 10 mmol) was added and the reaction mixture stirred overnight. The mixture was cooled to 0 °C and excess NaH was destroyed by a slow addition of water. The obtained suspension was extracted with EtOAc (3 × 40 mL), the organic phase was dried (Na_2SO_4) and evaporated under reduced pressure. The residue was purified by flash chromatography eluting with CH_2Cl_2/EtOAc 9.5/0.5 to 9/1 to yield **9** as a white foam (2.21 g; 85%). To an ice-cooled solution of **9** (2.16 g, 3.3 mmol) in dry CH_2Cl_2 (73 mL), CF_3COOH (0.73 mL; 9.82 mmol) was added and the reaction mixture was stirred for 2 min. The mixture was diluted with 10% (w/v) Na_2CO_3 aqueous solution and extracted with EtOAc (3 × 40 mL). The combined organic layers were washed with water (50 mL) and dried (Na_2SO_4) to afford a crude product which was purified by flash chromatography eluting with CH_2Cl_2/MeOH 9.5/0.5 to 8.5/1.5 to yield 1.17 g (87%) of **10** as a colorless oil. To a stirred solution of **10** (1.17 g; 2.84 mmol) and Boc-β-Ala(OH) (0.67 g; 3.54 mmol) in dry CH_2Cl_2 (20 mL) kept at 0 °C, DCC (0.73 g; 3.54 mmol) was added, the ice bath was removed, and the reaction was stirred at rt for 15 h. The reaction mixture was cooled to 0 °C, and the obtained precipitate was filtered and washed with cold (0 °C) CH_2Cl_2. The liquid phase was washed with water (3 × 30 mL) and brine (30 mL) and then dried and evaporated under reduced pressure to leave a white solid. The crude material was purified by flash chromatography eluting with CH_2Cl_2 + 2% MeOH, to give 1.60 g (97%) of **11** as a white foam. The obtained product was dissolved in CH_2Cl_2 (41 mL), treated with CF_3COOH (4.1 mL; 55 mmol), and stirred at rt for 20 h. The solvent was evaporated under reduced pressure, and the dark oily residue was treated with water (20 mL). The formed precipitate was filtered off through a sintered glass funnel, and the liquid phase was extracted with EtOAc (3 × 20 mL). The aqueous layer was evaporated under reduced pressure to leave 1.12 g (87%) of **12** as a colorless semisolid material. The product was recrystallized twice from dry MeOH/Et_2O and freeze-dried. ^{1}H NMR (CD_3OD): δ 8.74 (s, 1H, ImH_2), 7.3 (s, 1H, ImH_5), 4.33−4.29 (m, 1H, CH), 3.56−3.45 (m, 4H, 2 CH_2O), 3.15−3.11 (t, 2H, J = 6.6 Hz, CH_2NH_3^+), 3.07−2.87 (m, 2H, ImCH_2), 2.59 (t, 2H, J = 6.6 Hz, COCH_2), 1.19 (t, 3H, J = 6.9 Hz, CH_3). ^{13}C NMR (CD_3OD): δ 172.1, 134.9, 132.3, 118, 72.2, 67.8, 49.9, 37, 32.8, 27.9, 15.4.

Ionization Constants and Lipophilicity Descriptors. The ionization constants of compounds were determined by potentiometric titration with the GLpKa apparatus (Sirius Analytical Instruments Ltd, Forest Row, East Sussex, UK). Ionization constants of carnosine **1** and compounds **7a**−**g**, **7l**−**n**, and **12** were obtained by aqueous titrations by at least four separate titrations for each compound: different aqueous solutions (ionic strength adjusted to 0.15 M with KCl) of the compounds (20 mL, about 1 mM) were initially acidified to pH 1.8 with 0.5 N HCl; the solutions were then titrated with standardized 0.5 N KOH to pH 12.2. Because of the low aqueous solubility, ionization constants measurement of compounds **7h**−**i** required titrations in the presence of methanol as a cosolvent: at least five different hydro-organic solutions (ionic strength adjusted to 0.15 M with KCl) of the compounds (20 mL, about 1 mM in 20−34 wt % methanol) were initially acidified to pH 1.8 with 0.5 N HCl; the solutions were then titrated with standardized 0.5 N KOH to pH 12.2. The initial estimates of the p_sK_a values (the apparent ionization constants in the water−methanol mixtures) were obtained and aqueous pK_a values were determined by extrapolation to zero content of the cosolvent according to the Yasuda−Shedlovsky procedure.[51] All the titrations were performed under nitrogen at 25.0 ± 0.1 °C. The apparent partition coefficients log $D^{7.4}$ were obtained by shake-flask procedure at pH 7.4 (phosphate buffer solution with ionic strength adjusted to 0.15 M with KCl); *n*-octanol was added to the buffer, and the two phases were mutually saturated by shaking for 4 h. The compounds were solubilized in the buffered aqueous phase at a concentration of about 0.1 mM, and an appropriate amount of *n*-octanol was added. The two phases were shaken for about 20 min, by which time the partitioning equilibrium of solutes was reached and then centrifuged (10000 rpm, 10 min). The concentration of the solutes in the aqueous phase was measured by UV spectrophotometer (UV-2501PC, Shimadzu) at 230 nm. For each compound, at least seven log D values were measured.

Copper Complexes. The complex formation between copper(II) and carnosine and derivatives **7a**, **7d**, **7g**, **7l**, **7m**, and **12** was investigated by means of the classical pH-metric technique with the GLpKa apparatus. For each compound, at least three separate titrations were performed: different aqueous solutions of the compounds and of $CuCl_2$ equimolar (1 mM) were initially acidified to pH 1.8 with 0.5 N HCl; the solutions were then titrated with standardized 0.5 N KOH to pH 12.2. The measurements were carried out under nitrogen at 25.0 ± 0.1 °C and ionic strength adjusted to 0.15 M (KCl). The elaboration of experimental pH-metric data, in order to calculate the

values of formation constants, was performed by the BSTAC program.[30]

Stability in Human Serum. A solution of each compound (10 mM) in water was added to human serum (Sigma) preheated at 37 °C, and the final concentration of the compound was 0.5 mM. Resulting solutions were incubated at 37 ± 0.5 °C, and at appropriate time intervals, 500 μL of reaction mixture was withdrawn and added to 500 μL of acetonitrile containing 0.1% trifluoroacetic acid in order to deproteinize the serum. The sample was sonicated, vortexed, and then centrifuged for 10 min at 2150*g*. The clear supernatant was filtered by 0.45 μm PTFE filters (Alltech) and analyzed by RP-HPLC. HPLC analyses were performed with a HP 1100 chromatograph system (Agilent Technologies, Palo Alto, CA, USA) equipped with a quaternary pump (model G1311A), a membrane degasser (G1379A), and a diode-array detector (DAD) (model G1315B) integrated in the HP1100 system. Data analysis was done using a HP ChemStation system (Agilent Technologies). The analytical column was a Purospher C18-endcapped (250 mm × 4.6 mm, 5 μm particle size) (Merck Darmstadt, Germany). The mobile phase consisting of methanol/20 mM CH_3COONa pH 4.5−5 mM SDS (80/20 to 60/40 in accordance with the polarity of compounds), and the flow rate was 0.7 mL/min. The injection volume was 20 μL (Rheodyne, Cotati, CA). The column effluent was monitored at 210 and 223 nm referenced against a 360 nm wavelength. Quantitation was done by comparison of peak areas with standards chromatographed under the same conditions.

Antioxidant Activity. LDL Isolation and Oxidation. Human plasma from healthy donors was provided by Blood Bank (AO San Giovanni Battista Turin) and added with 0.1% EDTA. The LDL fraction was isolated by ultracentrifugation through NaCl discontinuous gradients and collected as the fraction floating at a density of 1.019−1.063 g/mL. The determination of the lag phase (t_{lag}) and of the propagation rate (R) was carried out as previously described.[52] EDTA was removed by rapid filtration through disposable desalting columns Econo-Pac 10 DG (Bio-Rad). Filtered LDL were diluted with PBS (10 mM phosphate buffer, pH 7.4) to give a final concentration of 50 μg of LDL protein/mL and transferred to a 1 cm cuvette with 50 μL of water alone or 50 μL of tested compound solution in water at a final concentration of 100 μM. The formation of conjugated dienes was measured spectrophotometrically in a Varian Cary 50 Bio spectrophotometer, equipped with a thermostatic control (37 °C) and an automatically exchangeable multipositions cuvettes holder, operating at 234 nm. Oxidation was initiated by the addition to the LDL suspension of $CuSO_4$ at a final concentration of 2.5 μM.

In Vitro HNE Scavenging Studies. HNE Incubation and LC Analysis. HNE (final concentration 50 μM in 1 mM phosphate buffer, pH 7.4) was incubated with solution of **7a**−**n**, **12**, or with carnosine (final concentration 1 mM in 1 mM phosphate buffer, pH 7.4) for different periods (up to 24 h) at 37 °C. Samples for each different incubation time were directly analyzed by HPLC to measure HNE consumption, as previously described.[6,49] HNE was determined by reverse-phase HPLC using a HP 1100 chromatograph system (Agilent Technologies, Palo Alto, CA, USA). Reaction mixture (20 μL) were eluted on a Agilent Zorbax Eclipse XDB-C18 column (150 mm × 4.6 mm; particle size 5 μm). The mobile phase was 60% A (water/acetonitrile/formic acid; 9:1:0.01, v/v/v) and 40% B (water/acetonitrile; 1:9, v/v) delivered at a flow rate of 1 mL/min. The column effluent was monitored at 223 nm.

Protection from HNE-Induced Cell Death. Cell Culture. All experiments were performed in accordance with the guidelines established by the National Council on Animal Care and approved by the local Animal Care Committee of Turin University. Hippocampal cells were obtained from black-six mouse 18-day embryos. The hippocampus was rapidly dissected under sterile conditions, kept in cold HBSS (4 °C) with high glucose, and then digested with papain (0.5 mg/mL) dissolved in HBSS plus DNAse (0,1 mg/mL). Isolated cells were plated onto Petri dishes, coated with poly-DL-lysine and laminine, at the final density of 260 cells/mm^2. The cells were incubated with 1% penicillin/streptomycin, 1% glutamax, 2% B-27 supplemented neurobasal medium in a humidified 5% CO_2 atmosphere at 37 °C for 6 days before performing the experiments.

Cytotoxicity Assays. Carnosine and **7d** were dissolved in the culture medium containing Neurobasal (Invitrogen), 2% B-27, 1% pen-strep (Lonza), and 1% ultraglutamine (Lonza) and used at the final concentration of 100 μM. HNE (Cayman) was stored at −80 °C in ethanol and then tested at the final concentration of 10 and 20 μM. After incubating hippocampal cells with the substances for 24 h, cell viability was determined by Trypan Blue exclusion, in order to stain just dead cells, due to loss of membrane integrity. Cells were counted with knowledge of the treatment history of the culture by comparing the number of living cells before incubation and after 24 h of treatment. Substances were tested alone and combined to HNE to assess not only the cytoprotective activity of carnosine and the carnosine analogue **7d** but also to exclude a possible toxicity of the compound. The percentage of cytoprotection was then evaluated by comparing the percentage of cells death after exposure to HNE and to HNE + **7d**. Data are given as the mean ± SEM for 4−7 experiments. Statistical significance was calculated by using Student's paired t test. Values of $p < 0.05$ were considered significant.

HPLC Detection of 7d in Rat Blood and Brain. Male Wistar rats weighing 200−250 g were used for this experiment. Each rat received 20 mg/kg of **7d** by iv injection of 200 μL of compound dissolved in 0.9% normal saline. After 1.5 or 3 h, animals were sacrificed for decapitation, and three rats were used for any time point. Blood was collected in polystyrene tubes with 500 UI eparine, and the brain was rapidly removed, rinsed with cold distilled water, weighed, and homogenized at 4 °C in an equal volume of cold distilled water using a Potter−Elvehjem homogenizer. An equal volume of acetonitrile containing 0.1% trifluoroacetic acid was added to blood samples or brain tissue homogenates to precipitate proteins. The samples were sonicated, vortexed, and then centrifuged for 10 min at 2150*g*. The clear supernatant was filtered by 0.45 μm PTFE filters and analyzed by RP-HPLC. HPLC analyses were performed with the same chromatograph system and stationary phase used for stability in human serum analyses. The supernatant (100 μL) was eluted with methanol/20 mM CH_3COONa pH 4.5 and 5 mM SDS (70/30) at a flow rate of 0.7 mL/min. The column effluent was monitored at 210 and 223 nm (reference 360 nm). Samples from untreated rats were used either as control or, after adding a known amount of **7d**, as standard.

Acknowledgment. This work was supported by Regione Piemonte, "Progetto di Ricerca Sanitaria Finalizzata", Bando Regionale 2009. The help from D. Dallorto and Dr. A. Barge in the brain-penetration experiments is gratefully acknowledged.

Supporting Information Available: Elemental analyses, HPLC and MS detection of **7d** in rat brain homogenate. This material is available free of charge via the Internet at http://pubs.acs.org.

References

(1) Boldyrev, A. A. *Carnosine and Oxidative Stress in Cells and Tissues*; Nova Science Publisher, Inc.: New York, 2006.
(2) Hipkiss, A. R. Carnosine, a protective, anti ageing peptide? *Int. J. Biochem. Cell Biol.* **1998**, *30*, 863–868.
(3) Hipkiss, A. R.; Preston, J. E.; Himsworth, D. T. M.; Worthington, V. C.; Keown, M.; Michaelis, J.; Lawrence, J.; Mateen, A.; Allende, L.; Eagles, P. A. M.; Abbott, N. J. Pluripotent Protective Effects of Carnosine, A Naturally Occuring Dipeptide. *Ann. N.Y. Acad. Sci.* **1998**, *854*, 37–53.

(4) Stvolinsky, S. L.; Dobrota, D. Anti-ischemic Activity of Carnosine. *Biochemistry* (*Moscow*) **2000**, *65*, 998–1005.

(5) Hipkiss, A. R. Could Carnosine or Related Structures Suppress Alzheimer Disease? *J. Alzheimer's Dis.* **2007**, *11*, 229–240and references therein .

(6) Aldini, G.; Carini, M.; Beretta, G.; Bradamante, S.; Maffei Facino, R. Carnosine is a quencher of 4-hydroxy-nonenal: through what mechanism of reaction? *Biochem. Biophys. Res. Commun.* **2002**, *298*, 699–706.

(7) Liu, Y.; Xu, G.; Sayre, L. M. Carnosine Inhibits (*E*)-4-Hydroxy-2-nonenal-Induced Protein Cross-Linking: Structural Characterization of Carnosine-HNE Adducts. *Chem. Res. Toxicol.* **2003**, *16*, 1589–1597.

(8) Guiotto, A.; Calderan, A.; Ruzza, P.; Borin, G. Carnosine and Carnosine-Related Antioxidants: A Review. *Curr. Med. Chem.* **2005**, *12*, 2293–2315.

(9) Bierhaus, A.; Hofman, M.; Ziegler, R.; Nawroth, P. P. AGEs and their interactions with AGE receptors in vascular disease and diabetes mellitus. 1. AGE concept. *Cardiovasc. Res.* **1998**, *37*, 586–600.

(10) Hipkiss, A. R.; Michaelis, J.; Syrris, P. Non-enzymatic glycosation of the dipeptide L-carnosine, a potential anti-protein-cross-linking agent. *FEBS Lett.* **1995**, *371*, 81–85.

(11) Hipkiss, A. R.; Brownson, C. A possible new role for the anti ageing peptide carnosine. *Cell. Mol. Life Sci.* **2000**, *57*, 747–753.

(12) Hobart, L.; Seibel, I.; Yeargans., G. S.; Seidler, N. W. Anti-cross-linking properties of carnosine: significance of histidine. *Life Sci.* **2004**, *75*, 1379–1389.

(13) Pegova, A.; Abe, H.; Boldyrev, A. Hydrolysis of carnosine and related compounds by mammalian carnosinases. *Comp. Biochem. Physiol., Part B: Biochem. Mol. Biol.* **2000**, *127*, 443–446and references therein .

(14) Lenney, J. F.; George, R. P.; Weiss, A. M.; Kucera, C. M.; Chan, P. W.; Rinzier, G. S. Human serum carnosinase: characterisation, distinction from cellular carnosinase, and activation by cadmium. *Clin. Chim. Acta* **1982**, *123*, 221–231.

(15) Vistoli, G.; Pedretti, A.; Cattaneo, M.; Aldini, G.; Testa, B. Homology Modeling of Human Serum Carnosinase, a Potential Medicinal Target, and MD Simulations of its Allosteric Activation by Citrate. *J. Med. Chem.* **2006**, *49*, 3269–3277.

(16) Pedretti, A.; De Luca, L.; Marconi, C.; Negrisoli, G.; Aldini, G.; Vistoli, G. Modeling of the Intestinal Peptide Transporter hPepT1 and Analysis of its Transport Capacities by Docking and Pharmacophore Mapping. *ChemMedChem* **2008**, *3*, 1913–1921.

(17) Kovalainen, J. T.; Christiaans, J. A. M.; Kotisaari, S.; Laitinen, J. T.; Männistö, P. T.; Tuomisto, L.; Gynther, J. Synthesis and in Vitro Pharmacology of a Series of New Chiral Histamine H_3-Receptor Ligands: 2-(*R* and *S*)-Amino-3-(1*H*-imidazol-4(5)-yl)propyl Ether Derivatives. *J. Med. Chem.* **1999**, *42* (7), 1193–1202.

(18) Babizhayev, M. A.; Courbebassie, Y.; Nicolay, J.-F.; Semiletov, Y. A. Design and biological activity of imidazole-containing peptidomimetics with a broad-spectrum antioxidant activity. *Lett. Pept. Sci.* **1998**, *5*, 163–169.

(19) Babyzhayev, M. A. Biological activities of the natural imidazole-containing peptidomimetics *n*-acetylcarnosine, carcinine and L-carnosine in ophthalmic and skin care products. *Life Sci.* **2006**, *78*, 2343–2357.

(20) Calcagni, A.; Ciattini, P. G.; Di Stefano, A.; Duprè, S.; Luisi, G.; Pinnen, F.; Rossi, D.; Spirito, A. $\Phi(SO_2NH)$ transition state isosteres of peptides. Synthesis and bioactivity of sulfonamido pseudopeptides related to carnosine. *Farmaco* **1999**, *54*, 673–677.

(21) Cacciatore, I.; Cocco, A.; Costa, M.; Fontana, M.; Lucente, G.; Pecci, L.; Pinnen, F. Biochemical properties of new synthetic carnosine analogues containing the residue of 2,3-diaminopropionic acid: the effect of *N*-acetylation. *Amino Acids* **2005**, *28*, 77–83.

(22) Attanasio, F.; Cataldo, S.; Fisichella, S.; Nicoletti, S.; Nicoletti, V. G.; Pignataro, B.; Savarino, A.; Rizzarelli, E. Protective Effects of L- and D-Carnosine on *R*-Crystallin Amyloid Fibril Formation: Implications for Cataract Disease. *Biochemistry* **2009**, *48*, 652–6531.

(23) Vistoli, G.; Orioli, M.; Pedretti, A.; Regazzoni, A.; Canevotti, R.; Negrisoli, G.; Carini, M.; Aldini, G. Design, synthesis, and evaluation of carnosine derivatives as selective and efficient sequestering agents of cytotoxic reactive carbonyl species. *ChemMedChem.* **2009**, *4*, 1–10.

(24) La Mendola, D.; Sortino, S.; Vecchio, G.; Rizzarelli, E. Synthesis of New Carnosine Derivatives of β-Cyclodextrin and Their Hydroxyl Radical Scavenger Ability. *Helv. Chim. Acta* **2002**, *85*, 1633–1643.

(25) Bellia, F.; Amorini, A. M.; La Mendola, D.; Vecchio, G.; Tavazzi, B.; Giardina, B.; Di Pietro, V.; Lazzarino, G.; Rizzarelli, E. New glycosidic derivatives of histidine-containing dipeptides with antioxidant properties and resistant to carnosinase activity. *Eur. J. Med. Chem.* **2008**, *43*, 373–380.

(26) Hamdoune, F.; El Moujahid, C.; Rodehuser, L.; Gerardin, C.; Henry, B.; Stebe, M.; Amos, J.; Marraha, M.; Asskali, A.; Selve, C. Amphiphilic and cation-complexing compounds based on peptidoamines. *New J. Chem.* **2000**, *24*, 1037–1042.

(27) Baran, E. J. Metal complexes of carnosine. *Biochemistry* (*Moscow*) **2000**, *75*, 928–937.

(28) Daniele, P. G.; Prenesti, E.; Zelano, V.; Ostacoli, G. Chemical relevance of the copper(II)−L-carnosine system in aqueous solution: a thermodynamic and spectrophotometric study. *Spectrochim. Acta, Part A* **1993**, *9*, 1299–1306.

(29) Shen, J.; Li, Y.-Z.; Zhang, D.-M.; Chen, J.-H. Diaquabis[μ_2-3-(1*H*-imidazol-5-yl)-2-(3-iminopropionamido)propionate-κ^4 *N:N′,N″, O*]dicopper(II) dihydrate. *Acta Crystallogr., Sect. E: Struct. Rep. Online* **2007**, *63*, m2569–m2570.

(30) De Stefano, C.; Mineo, P.; Rigano, C.; Sammartano, S. Ionic strength dependence of formation constants. XVII. The calculation of equilibrium concentrations and formation constants. *Ann. Chim.* (*Rome*) **1993**, *83*, 243–277.

(31) Eberhardt, M. K. *Reactive Oxygen Metabolites*; CRC Press: Boca Raton, FL, 2000.

(32) Sayre, L. M.; Perry, G.; Smith, M. A. Oxidative Stress and Neurotoxicity. *Chem. Res. Toxicol.* **2008**, *21*, 172–188.

(33) Hayashi, T.; Shisido, N.; Nakayama, K.; Nunomura, A.; Smith, M. A.; Perry, G.; Nakamura, M. Lipid peroxidation and 4-hydroxy-2-nonenal formation by copper ion bound to amyloid-β peptide. *Free Radical Biol. Med.* **2007**, *43*, 1552–1559.

(34) Bennet, S.; Grant, M. M.; Aldred, S. Oxidative Stress in Vascular Dementia and Alzheimer's Disease: A Common Pathology. *J. Alzheimer's Dis.* **2009**, *17*, 245–257.

(35) Aldred, S.; Bennet, S.; Mecocci, P. Increased low-density lipoprotein oxidation, but not total plasma protein oxidation, in Alzheimer's disease. *Clin. Biochem.* **2010**, *43*, 267–271.

(36) Li, L.; Willets, R. S.; Polidori, M. C.; Stahl, W.; Nelles, G.; Sies, H.; Griffiths, H. R. Oxidative LDL modification is increased in vascular dementia and is inversely associated with cognitive performance. *Free Radical Res.* **2010**, *44*, 241–248.

(37) Bogardus, S. L.; Boissonneault, G. A. Carnosine inhibits in vitro low density lipoprotein oxidation. *Nutr. Res.* (*N. Y., NY, U.S.*) **2000**, *20*, 967–976.

(38) Pinchuk, I.; Lichtenberg, D. The mechanism of action of antioxidants against lipoprotein peroxidation, evaluation based on kinetic experiments. *Prog. Lipid Res.* **2002**, *41*, 279–314.

(39) Kuzuya, M.; Yamada, K.; Hayashi, T.; Funaki, C.; Naito, M.; Asai, K.; Kuzuya, F. Role of lipoprotein−copper complex in copper-catalysed peroxidation of low-density lipoprotein. *Biochem. Biophys. Acta* **1992**, *1123*, 334–341.

(40) Patel, R. P.; Svistunenko, D.; Wilson, M. T.; Darley-Usmar, V. M. Reduction of Cu(II) by lipid hydroperoxides: implications for the copper-dependent oxidation of low density lipoprotein. *Biochem. J.* **1997**, *322*, 425–433.

(41) Mark, R. J.; Lovell, M. A.; Markesbery, W. R.; Uchida, K.; Mattson, M. P. A role for 4-hydroxynonenal, an aldehydic product of lipid peroxidation, in disruption of ion homeostasis and neuronal death induced by amyloid betapeptide. *J. Neurochem.* **1997**, *68*, 255–264.

(42) Butterfield, D. A.; Castegna, A.; Lauderback, C. M.; Drake, J. Evidence that amyloid beta-peptide-induced lipid peroxidation and its sequelae in Alzheimer's disease brain contribute to neuronal death. *Neurobiol. Aging* **2002**, *23*, 655–664.

(43) Rabacchi, S. A.; Friedman, W. J.; Shelanski, M. L.; Troy, C. M. Divergence of the apoptotic pathways induced by 4-hydroxynonenal and amyloid beta-protein. *Neurobiol. Aging* **2004**, *25*, 1057–1066.

(44) Keller, J. N.; Hanni, K. B.; Markesbery, W. R. 4-Hydroxynonenal increases neuronal susceptibility to oxidative stress. *J. Neurosci. Res.* **1999**, *58*, 823–830.

(45) Ando, Y.; Brannstrom, T.; Uchida, K.; Nyhlin, N.; Nasman, B.; Suhr, O.; Yamashita, T.; Olsson, T.; El Salhy, M.; Uchino, M.; Ando, M. Histochemical detection of 4-hydroxynonenal protein in Alzheimer amyloid. *J. Neurol. Sci.* **1998**, *156*, 172–176.

(46) Sayre, L. M.; Zelasko, D. A.; Harris, P. L.; Perry, G.; Salomon, R. G.; Smith, M. A. 4-Hydroxynonenal-derived advanced lipid peroxidation end products are increased in Alzheimer's disease. *J. Neurochem.* **1997**, *68*, 2092–2097.

(47) Takeda, A.; Smith, M. A.; Avila, J.; Nunomura, A.; Siedlak, S. L.; Zhu, X.; Perry, G.; Sayre, L. M. In Alzheimer's disease, heme oxygenase is coincident with Alz50, an epitope of tau induced by

4-hydroxy-2-nonenal modification. *J. Neurochem.* **2000**, *75*, 1234–1241.
(48) Carini, M.; Aldini, G.; Beretta, G.; Arlandini, E.; Maffei Facino, R. Acrolein-sequestring ability of endogenous dipeptides: characterisation of carnosine and homocarnosine/acrolein adducts by electrospray ionization tandem mass spectrometry. *J. Mass Spectrom.* **2002**, *38*, 996–1006.
(49) Beretta, G.; Artali, R.; Regazzoni, L.; Panigati, M.; Maffei Facino, R. Glycyl-histidyl-lysine (GHK) is a quencher of α,*β*-4-hydroxy-*trans*-2-nonenal: a comparison with carnosine. Insights into the mechanism of reaction by electrospray ionization mass spectrometry. ^{1}H NMR, and computational techniques. *Chem. Res. Toxicol.* **2007**, *20*, 1309–1314.
(50) Otani, H.; Okumura, n.; Hashida-Okumura, A.; Nagai, K. Identification and Characterization of a Mouse Dipeptidase That Hydrolyzes L-Carnosine. *J. Biochem.* **2005**, *137*, 167–175.
(51) Avdeef, A.; Comer, J. E. A.; Thompson, S. J. pH-Metric log P.3. Glass electrode calibration in methanol-water, applied to pK_a determination of water-insoluble substances. *Anal. Chem.* **1993**, *65*, 42–49.
(52) Esterbauer, H.; Striegl, G.; Puhl, H.; Rotheneder, M. Continuous monitoring of in vitro oxidation of human low density lipoprotein. *Free Radical Res. Commun.* **1989**, *6*, 67–75.
(53) Daniele, P. G.; Amico, P.; Ostacoli, G. Heterobinuclear copper(II)−L-carnosine complexes with cadmium(II) and zinc(II) in aqueous solution. *Inorg. Chim. Acta* **1982**, *66*, 65–70.